JOURNAL OF SPACECRAFT AND ROCKETS
Vol. 33, No. 4, July–August 1996

Multipayload Modeling for the Upper Atmosphere Research Satellite

C. R. Larson*
Rockwell International, Downey, California 90241-7009
S. E. Woodard†
NASA Langley Research Center, Hampton, Virginia 23681-0001
and
L. Tischner,‡ E. Tong,* M. Schmidt,§ J. Cheng,§ E. Fujii,¶ and S. Ghofranian**
Rockwell International, Downey, California 90241-7009

A multipayload spacecraft modeling approach that combines constituent subassemblies (plant and controllers) into a combined system (model synthesis) is presented. This technique was used to model the Upper Atmosphere Research Satellite. The simulation was developed to determine the amount of controls–structure interaction, and the satellite flight results verified simulation predictions during payload tracking and scan modes and solar-array sun-tracking modes. The simulation was developed using the Dynamics Analysis Design System program. The program was modified to include a multirate sampling capability, a robust analog delay element, a stepper-motor kinematic driver, and a modified flexible body formulation. The simulation includes the structural models of the satellite components, the dominant flexible modes, the vehicle attitude control system and orbit adjust capability, and all instrument elevation and azimuth control systems. The model includes the flexible modes below 16 Hz and the instrument control systems. This study presented simulation results using the synthesized modeling approach and the in-flight data to validate the approach

Introduction

NASA Langley's Controls–Structure Interaction (CSI) Program has used in-flight data from the Upper Atmosphere Research Satellite (UARS), launched Sept. 12, 1991, for validating spacecraft modeling and analysis methodology.[1–3] The study consisted of three major activities: telemetry acquisition and analysis; two in-flight experiments performed on May 1, 1992, and Sept. 17, 1993, which provided data cases to be used expressly for the study (approximately three orbits each); and an evaluation of dynamic simulation models of UARS with flight telemetry. The goal of the study is to advance design and analysis technology to better predict spacecraft pointing jitter so that adequate (but not excessive) design margins are used to assure mission success. Jitter is the measure of the excursion of an instrument's boresight in a reference time interval such as a sampling time period.[4] By examining in-orbit UARS data to determine whether prelaunch spacecraft jitter predictions were accurate for both single and multiple disturbance sources on the spacecraft, one can ascertain how good the design methodology that was used before launch is and what improvements can be made. Furthermore, the in-flight data can be used for validating other design methodologies.

This paper presents a case study in CSI for a variety of payloads with in-flight verification. The technique uses a synthesis approach to modeling an overall system. Each subassembly is modeled separately. The subassembly modeling includes the plant (i.e., physical model of an instrument or subsystem) and its controller. All subassemblies are combined into a single system. The result is a simulation model that will allow the designer to examine the influence that each component has on the overall system as well as the mutual interactions that the components have on each other. Therefore, using the approach, it is possible to examine payload–payload interaction and structure–payload interaction. Structure–payload interaction is the effect that a spacecraft's vibration has on an instrument's line-of-sight pointing. Thus it becomes possible to ascertain if the interactions will have any adverse effect on payload measurements. Traditional disturbance analysis is also a capability of this modeling technique. The modeling approach also includes nonlinear translational and rotational dynamics.

Satellite Description

The satellite is shown attached to the Space Shuttle Discovery (STS-48) bay in Fig. 1. The in-orbit deployed configuration is shown in Fig. 2. The UARS observatory includes ten science instruments mounted on an Instrument Module (IM), which is affixed to a Multimission Modular Spacecraft (MMS). The MMS provides attitude control using the reaction-wheel assembly,[5–7] communication and data handling, electrical power distribution, and propulsion. A high-gain antenna provides forward and return communication links to the two Tracking and Data Relay Satellites.[5,6] A Solar Stellar Pointing Platform (SSPP) and six solar array panels on a single sail are also attached to the instrument module.[5,6]

Since many of the UARS instruments or subsystems are gimbaled, during the course of an orbit many disturbances can be imparted to the platform, which include impulses and ramped and

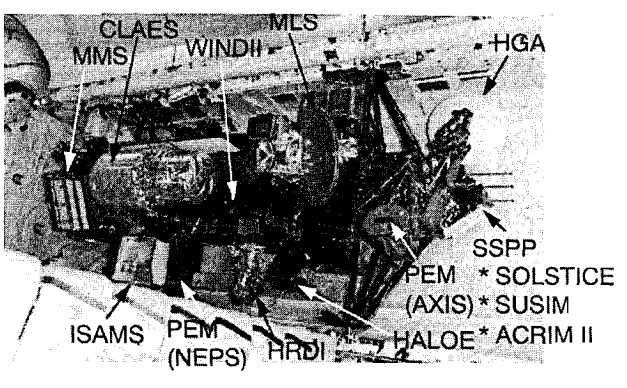

Fig. 1 UARS in the bay of the Space Shuttle Discovery (STS-48).

Received Jan. 2, 1995; presented as Paper 95-0622 at the AIAA 33rd Aerospace Sciences Meeting, Reno, NV, Jan. 9–12, 1995; revision received Nov. 6, 1995; accepted for publication Nov. 10, 1995.

*Senior Engineering Specialist, Vehicle and System Analysis.
†Aerospace Engineer, Structural Dynamics Branch. Member AIAA.
‡Engineering Specialist, Vehicle and System Analysis.
§Member, Technical Staff, Avionics.
¶Engineering Specialist, Avionics.
**Principal Engineering Specialist, Vehicle and System Analysis.

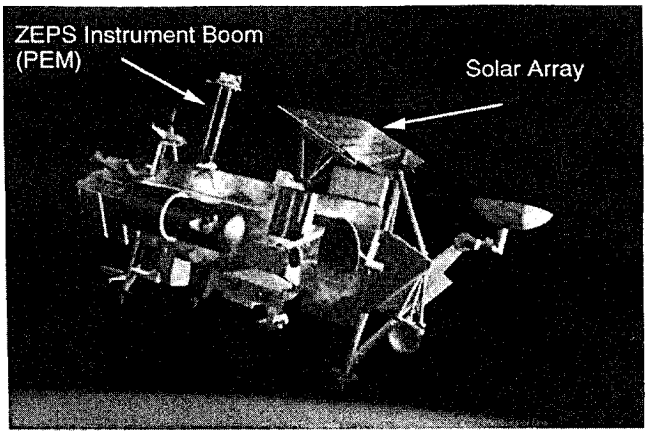

Fig. 2 Artist's conception of the UARS on orbit.

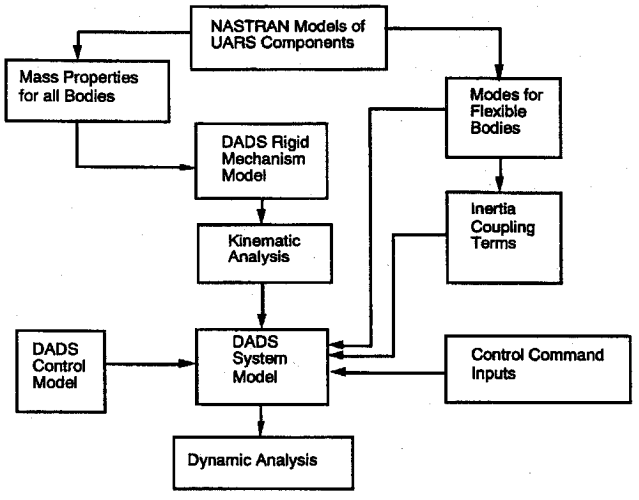

Fig. 3 UARS modeling architecture.

periodic disturbances.[1–4,7–12] The satellite has two elastic flexible appendages—the solar array and an instrument boom containing the Zenith Energetic-Particle System (ZEPS)—which can be excited by multiple disturbance sources on-board the spacecraft.

The UARS simulation includes the structural models, the flexible modes below 16 Hz, the residual flexibility for each gimbal degree of freedom, and the control systems for the attitude control system, the high-gain antenna, the High-Resolution Doppler Imager, the SSPP, and the solar arrays. The Solar Ultraviolet Spectral Irradiance Monitor and the Solar–Stellar Irradiance Comparison Experiment instruments are mounted on the SSPP. The Microwave Limb Sounder (MLS) disturbance and the Halogen Occultation Experiment (HALOE) scan, slew, and track modes are modeled. The MMS, the Wind Imaging Interferometer, the Improved Stratospheric and Mesospheric Sounder, and the Cryogenic Limb Array Etalon Spectrometer do not move, or their motion is insignificant; therefore, these payloads were considered to be rigidly attached to the IM truss structure. The flexibility and inertia properties up to the first gimbal are included as bases for the various components in the instrument module. The components beyond the first gimbal are considered to be rigid. There were 13 flexible instrument-module modes (including the ZEPS boom) and 20 solar-array modes with frequencies below 16 Hz.

Because of space limitations, the only results presented in this paper are the development, simulation, and validation of the MLS antenna scans, HALOE solar scan and tracking, and solar-array drive dynamics.

Model Synthesis

The technique presented in this paper consists of combining individual components of the overall system and their controllers into a single system. The architecture for doing so is shown in Fig. 3. The model was developed using the Dynamic Analysis Design System (DADS) version 6.5 simulation program.[13] Each individual component is modeled in NASTRAN[14] as a finite element model. NASTRAN dynamic analysis produces a mass matrix, stiffness matrix, eigenvectors, and eigenvalues. The mass properties (mass and inertia) are used to model rigid mechanisms. DADS uses modal superposition to perform flexible dynamic analysis and uses the eigenvalues and eigenvectors to produce inertia coupling terms. Controllers for individual components are developed using control elements created with the simulation program. Other control commands can be included using user algorithms or user defined subroutines. All control models, kinematic drivers, subsystem flexibility, and inertia coupling are combined in the DADS simulation model, which produces a combined dynamical analysis of all components and controllers. This modeling technique allows one to examine the interaction of payloads, the influence that spacecraft vibration has on payload line-of-sight pointing, and the effect that payload motion has on the overall dynamic response.

Modifications of the DADS Simulation

The equations of motion for a flexible body can be derived using a variational approach.[15] Although the full equations of motion as presented in Ref. 15 and as programmed in DADS allow for changes in rigid-body mass properties, Coriolis acceleration, and centripetal forces, in most applications these are second-order terms and can be neglected. In the UARS model, since those second-order terms only increase the run time and do not contribute to the solution, they were eliminated from the model with no loss in accuracy.

The DADS generic program was modified to include a multirate sample-and-hold capability, an analog and digital delay element, and a stepper-motor kinematic driver. A multirate sample-and-hold logic was implemented in a user-defined subroutine. The sample and hold was necessary because the subsystems have different sampling rates. The least-common-multiple sampling period of 0.128 s was used to drive the sample-and-hold logic. A dummy input element with the digital flag set to true was used to force the integrator to stop on sampling intervals. The sampling rate was defined by the reciprocal of base sampling period. The generic DADS delay element failed when digital elements were present, which prompted the development of a new, robust delay element that is compatible with any type of control element. In the modified delay element, the historical array of delayed data increased from 500 past time steps to 2500 steps. First-in, first-out logic was used to develop the customized code. In view of the variable-step integration algorithm, a linear interpolation scheme was used to properly define the delayed output.

UARS Simulation Results

MLS

The MLS antenna scans the vertical profile of the atmosphere. The scan cycle of 65.5 s consists of a forward limb-viewing trace followed by a rewind. The MLS disturbance was modeled as a torque profile applied to an unconstrained joint.[8,9] A stepper motor controls the instrument motion. In the absence of flexibility and any other disturbances in the system, conservation of momentum is easily achieved at the instrument gimbal, making it unnecessary to constrain the joint between motor steps. However, when flexibility and external disturbances are present in the system, it becomes necessary to constrain the joint to ensure that the instrument's attitude is properly maintained. To accurately describe the MLS disturbance, an inverse dynamic approach was taken by modeling the stepper motor as a kinematic driver. This approach was equivalent to an ideal control system. The MLS flight scan was accurately represented by a closed-form solution of displacement, velocity, and acceleration. The implementation showed that the stepper-motor function was accurately represented, and the torque necessary to enforce the instrument movement was equivalent to torque profiles used by General Electric (UARS prime contractor).

When the MLS scan profile was used with an inactive UARS attitude control system, a drift in the UARS roll angle and the MLS antenna position was encountered. Figure 4a shows that a small

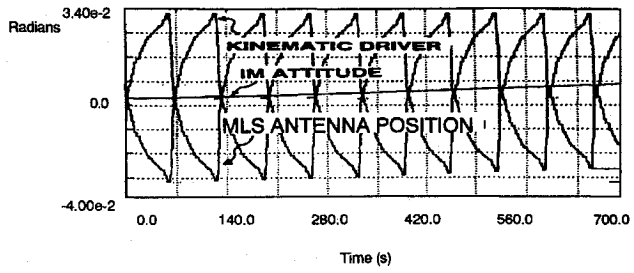

a) MLS antenna position: UARS simulation

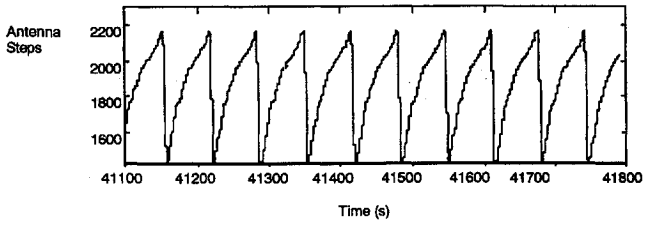

b) MLS antenna steps: day 301 after launch

Fig. 4 MLS simulated kinematic driver compared with in-flight history of MLS antenna steps.

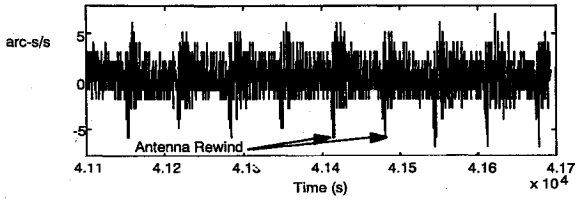

a) Roll attitude response: day 301 past launch of UARS

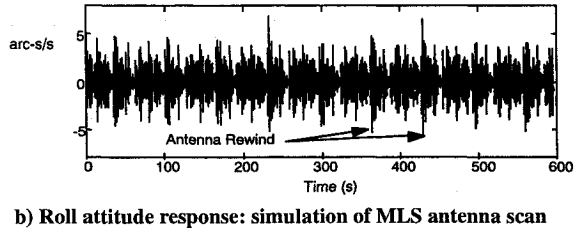

b) Roll attitude response: simulation of MLS antenna scan

Fig. 5 Roll attitude response to MLS simulated kinematic driver compared with in-flight roll attitude response to MLS antenna scanning and rewinding.

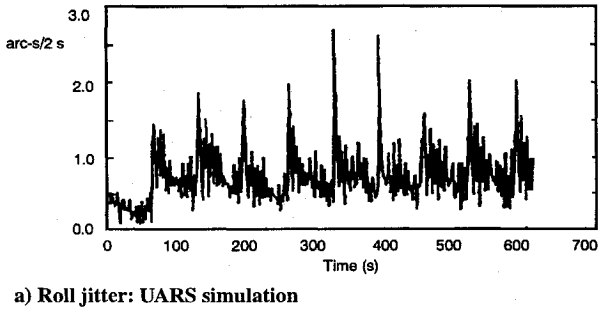

a) Roll jitter: UARS simulation

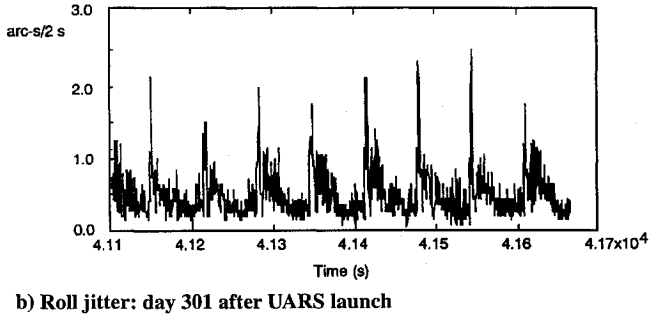

b) Roll jitter: day 301 after UARS launch

Fig. 6 Roll jitter derived from simulation of roll response to MLS scans, compared with that observed using in-flight data.

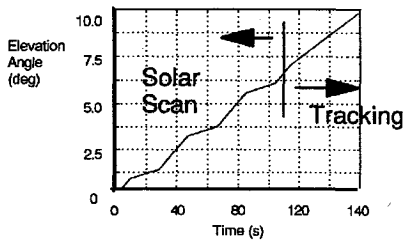

a) Simulation of HALOE scanning

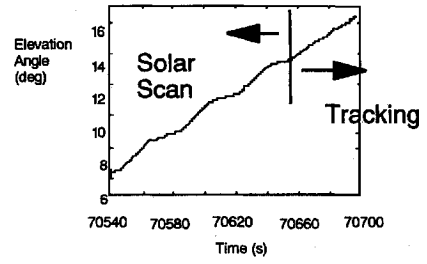

b) HALOE elevation during solar scan on May 1, 1992

Fig. 7 HALOE elevation history using DADS modeling compared with HALOE in-flight elevation history.

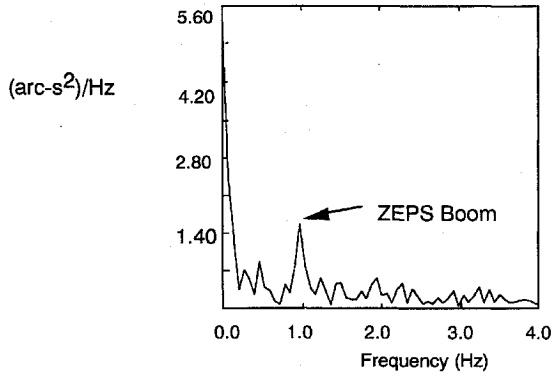

a) Frequency response of UARS to HALOE tracking sun

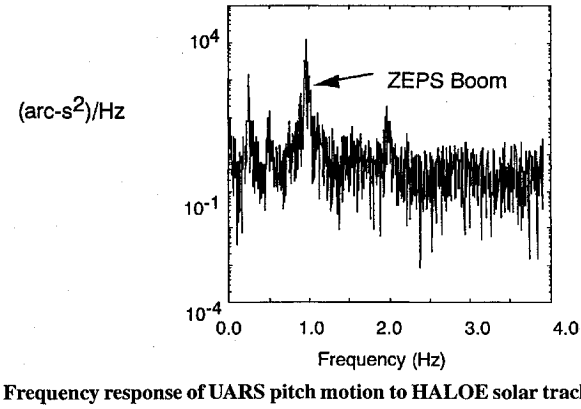

b) Frequency response of UARS pitch motion to HALOE solar tracking

Fig. 8 Simulated and in-flight pitch attitude frequency response to HALOE tracking.

(0.29-deg) drift in the UARS roll attitude over a 700-s period. The DADS results can also be compared with the in-flight time record of the MLS antenna. The total excursion for the in-flight data is measured by motor position steps and is 1.32 deg for 800 motor steps (1400 through 2200 in Fig. 4b). The simulated flight scan mode has 28 discrete displacements due to forward pulses and 2 discrete displacements due to return pulses. The simulation profile used to position the MLS antenna has an identical shape to that observed from flight data.

The response of the MLS antenna scan is shown in Fig. 5. The dominant spikes are a result of the rewind of the antenna. Both the simulated response and the measured response have peak values of 5–8″/s (magnitude). Furthermore, the response decay after the

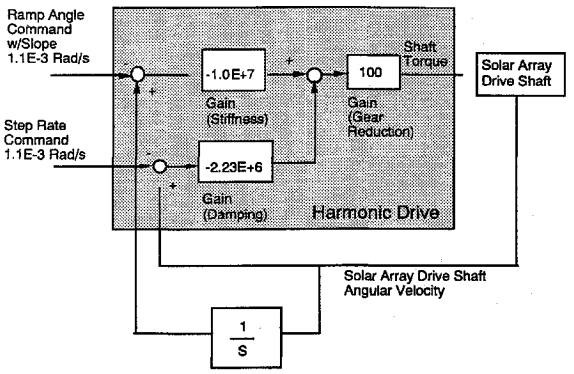

Fig. 9 Solar-array drive-shaft control.

spikes have similar trends. The measured jitter from the response is shown in Fig. 6. In both cases, the peak jitter was approximately 2.5″ for a 2-s window.

HALOE

A stepper-motor-driven biaxial gimbal system, fine and coarse sun sensors, and microprocessor-based closed-loop feedback sun-tracking control logic are used to maintain the HALOE's instantaneous field of view. The biaxial gimbal assembly contains independently controlled gimbals. Coarse and fine sun sensors provide error signals to the control algorithm.

HALOE autonomously performs solar acquisition, solar-scan calibration, track, and stow sequences during orbital sunrise and sunset. Unless commanded otherwise, HALOE alternates between sunrise and sunset sequences. The motor is assumed to respond to pulse

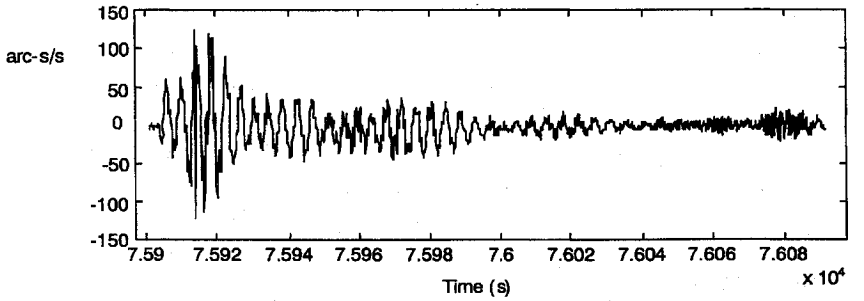

a) Roll attitude response to solar array rotation on day 265 past UARS launch

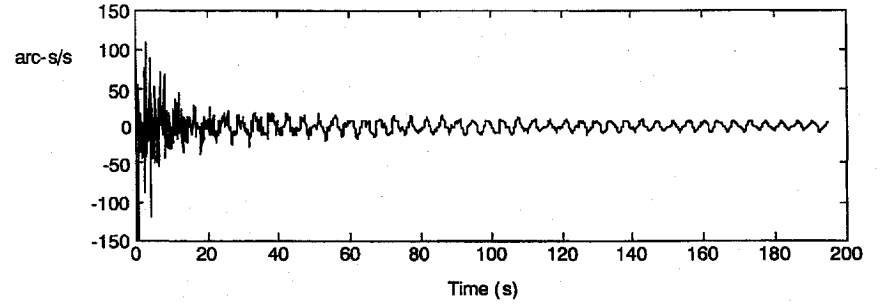

b) Roll attitude response to solar array rotation during simulation

Fig. 10 Comparison of simulated and in-flight roll attitude response to start of solar-array tracking.

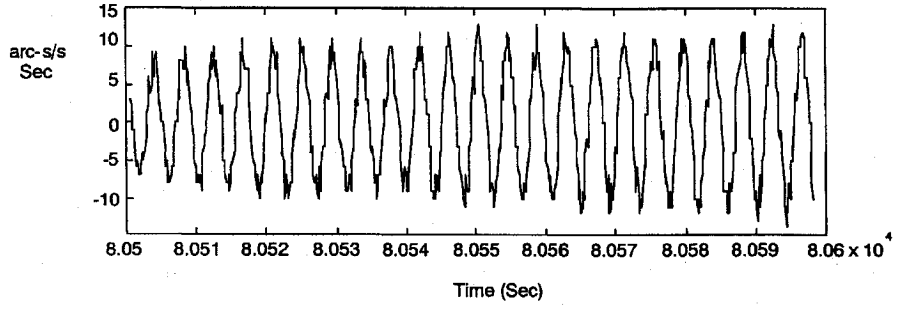

a) Roll attitude response to solar array rotation on day 233 past UARS launch

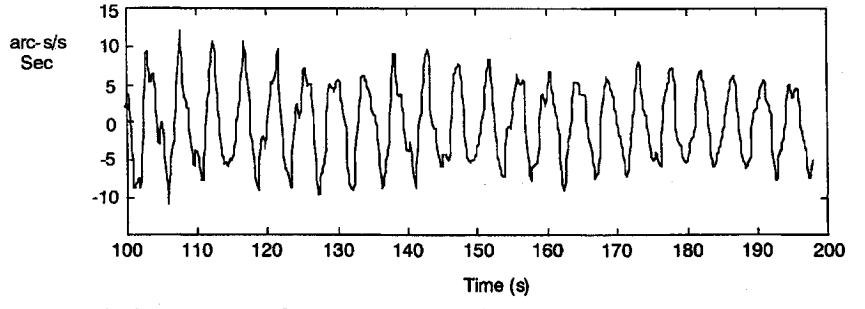

b) Roll attitude response to solar array rotation during simulation

Fig. 11 Simulated and in-flight roll attitude response during period in which solar-array drive is sole disturbance source.

commands with an instantaneous change in output-shaft angle rate to a preset value. The gear train and harmonic drive are modeled using control elements of DADS, and backlash and friction are neglected. The harmonic-drive compliance is modeled as a spring–mass system with viscous damping.

Figure 7a shows the results of modeling HALOE's solar scan and solar tracking. Because the simulated scanning and tracking compares favorably with that using the flight data from May 1, 1992, the elevation control system modeling has been verified. Figure 8 shows the frequency content of the pitch attitude response for both the flight data and the simulation. The DADS simulation data showed a peak at 1 Hz. That means the HALOE tracking mode can excite the ZEPS boom natural frequencies of 0.8 and 0.9 Hz. The UARS flight data (Fig. 7b) showed that the ZEPS boom was indeed excited during HALOE tracking.

Solar-Array Drive

The solar-array control system is an open-loop controller with a stepper motor, gearbox, and harmonic drive. The stepper motor is assumed to follow a constant-rate command. The backlash and friction in the gear train are assumed negligible. The harmonic-drive compliance is modeled as a spring–mass system with viscous damping. Figure 9 shows the solar-array drive controller.

The simulation of the solar-array drive was compared for two cases. The first case, Fig. 10, consists of the solar-array drive starting to rotate. The in-flight record is from June 2, 1992 (265 days after launch). Both the simulation and the flight data show the initial increase in the response of approximately 110″/s about the roll axis. Both cases also show the excitation of the 0.25-Hz modes. The second case of comparison is when the solar array has been on and all response transients are gone. The May 1, 1992 (233 days after launch), disturbance experiment provided a case where the solar array was the sole disturbance source. Both the simulated and the in-flight roll response, shown in Fig. 11, have approximately the same peak response of 10″/s (magnitude). Both also show excitation of the 0.25-Hz solar-array mode. Therefore, the modified solar-array drive controller accurately reflects the dynamics of the actual drive mechanism.

Conclusion

A multipayload spacecraft modeling approach that combines constituent subassemblies (plant and controllers) into a system (model synthesis) has been presented. This technique was used to model the UARS. A simulation was developed that determines the amount of CSI, and the UARS flight results verified simulation predictions during HALOE tracking, MLS scan mode, and solar-array sun-tracking mode. Many simulation obstacles were encountered and overcome. The simulation is currently being used by the NASA Langley Research Center.

Acknowledgments

The simulation was developed by Rockwell under NASA Contract NAS1-19243. The in-flight data acquisition and spacecraft disturbance and response studies were conducted by NASA Langley Research Center. The solar-array control system was based on information provided by General Electric Astro Space Division.

References

[1]Woodard, S. E., Garnek, M., Molnar, J. D., and Grantham, W. L., "The Upper Atmosphere Research Satellite Jitter Study," Flight Experiments Technical Interchange Meeting, Monterey, CA, Oct. 1992.

[2]Molnar, J., and Garnek, M., "UARS In-Flight Jitter Study for EOS," NASA CR 191419, Jan. 1993.

[3]Butterfield, A. J., and Woodard, S. E., "Payload–Payload Interaction and Structure–Payload Interaction Observed on the Upper Atmosphere Research Satellite," American Astronomical Society, Paper 93-551, Aug. 1993.

[4]Neste, S. L., "UARS Pointing Error Budgets," General Electric Co. Astro-Space Div., PIR U-1K21-UARS-517, July 1986.

[5]Anon., "Upper Atmosphere Research Satellite Project Data Book," General Electric Co. Astro-Space Div., NASA Goddard Space Flight Center, April 1987.

[6]Anon., "Upper Atmosphere Research Satellite Command and Telemetry Handbook," General Electric Co. Astro-Space Div., SDS-4219, Jan. 1991.

[7]Harding, R. R., "The Normal Mode Control Law for UARS," General Electric Co., Paper PIR U-1K21-UARS-336, Feb. 1986.

[8]Mills, R., and Garnek, M., "UARS Dynamic Disturbance Toque Analysis," General Electric Co., Paper PIR U-1K21 UARS 279, PIR U-1R44-UARS-1351, Nov. 1985.

[9]Sheldon, K. M., " Disturbance Torque Summary for UARS," General Electric Co., Paper PIR U-1K21-UARS-232, Sept. 1985.

[10]Zimbelman, D. F., "Thermal Elastic Shock and Its Effect on Topex Spacecraft Attitude Control," American Astronomical Society, Paper 91-055, Feb. 1991.

[11]Keafer, L. S., Sullivan, E. M., Spiers, R. B., Moore, A. S., Stump, C. W., Hardesty, C. A., Beswick, A. G., Baker, R. L., Smith, D. M., and Costulis, J. A., "Halogen Occultation Experiment Instrument Description Document," HALOE-02-028C, NASA, Oct. 1988.

[12]Sullivan, E. M., "HALOE Flight Operations Mode Document," HALOE-10-664, NASA, Feb. 1991.

[13]Anon., *Dynamic Analysis and Design System User's Guide*, Computer Aided Design Software, Inc., 1993.

[14]Anon., *MSC/NASTRAN Handbook for Dynamic Analysis*, MacNeal Schwendler Corp., 1983.

[15]S. Wu, E. J. Haug, and S. Kim, "A Variational Approach to Dynamics of Flexible Multibody Systems," *Mechanics of Structures and Machines*, Vol. 17, No. 1, 1989, pp. 3–32.

H. R. Anderson
Associate Editor